

## Chapter 2

### *Design of Sequence-Specific DNA Binding Molecules for DNA Methyltransferase Inhibition*

The text of this chapter is taken in part from a manuscript co-authored with Jordan L. Meier and Peter B. Dervan (California Institute of Technology).

(Kang, J. S.; Meier, J. L.; Dervan, P. B. *J. Am. Chem. Soc.* **2014**, *136*, 3687-3694.)

**Abstract**

The CpG dyad, an important genomic feature in DNA methylation and transcriptional regulation, is an attractive target for small molecules. To assess the utility of minor groove binding oligomers for CpG recognition, we screened a small library of hairpin pyrrole-imidazole polyamides targeting the sequence 5'-CGCG-3' and assessed their sequence specificity using an unbiased next-generation sequencing assay. Our findings indicate that hairpin polyamide of sequence PyIm $\beta$ Im- $\gamma$ -PyIm $\beta$ Im (**1**), previously identified as a high affinity 5'-CGCG-3' binder, favors 5'-GCGC-3' in an unanticipated reverse binding orientation. Replacement of one  $\beta$  alanine with Py to afford PyImPyIm- $\gamma$ -PyIm $\beta$ Im (**3**) restores the preference for 5'-CGCG-3' binding in a forward orientation. The minor groove binding hairpin **3** inhibits DNA methyltransferase activity in the major groove at its target site more effectively than **1**, providing a molecular basis for design of sequence-specific antagonists of CpG methylation.

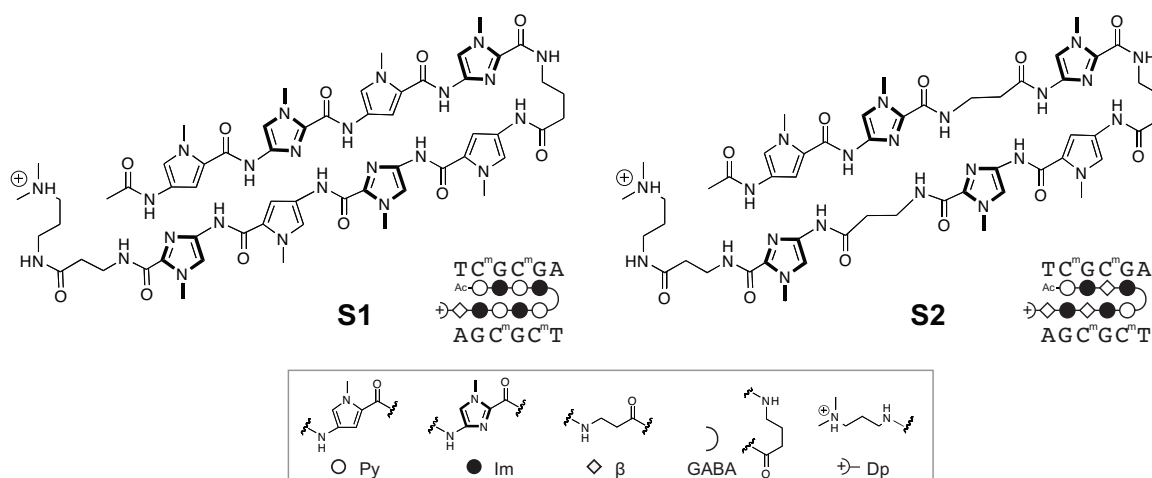
## 2.1 Introduction

The role of epigenetic dysregulation in cancer has motivated interest in DNA methylation and methods for its modulation.<sup>1,2</sup> In mammals, DNA methylation occurs in the major groove of DNA at the 5' position of both cytosine residues in the palindromic CG dyad (CpG). CpG's are rare in the genome and 70% methylated, with nearly all unmethylated CpG's clustered in G,C-rich regions called "CpG islands".<sup>3</sup> Approximately 60% of RNA Polymerase II transcribed human genes contain CpG islands,<sup>4</sup> and their methylation causes transcriptional repression.<sup>5</sup> In cancer, for example, otherwise functional tumor suppressor genes can be silenced by hypermethylation in their associated CpG island.<sup>6</sup> Importantly, inhibition of DNA methylation at tumor suppressor genes has been shown to reactivate apoptotic pathways and sensitize cancer cells to previously ineffective chemotherapy.<sup>7,8</sup>

The most effective demethylation agents are cytidine analogs such as 5-aza-deoxycytidine, which find limited use due to significant side effects.<sup>1</sup> These cytidine analogs are suicide inhibitors incorporated into DNA to form covalent methyltransferase-DNA adducts.<sup>9</sup> The methyltransferase is sequestered and unavailable to methylate CpG's, resulting in genome-wide demethylation. DNA binding molecules, such as the bis-intercalating natural product echinomycin,<sup>10</sup> can disrupt CpG methylation *in vitro* but have dose-limiting toxicities that have abrogated further clinical advancement.<sup>11</sup> While other CpG methylation inhibitors are under investigation,<sup>12-14</sup> none of these agents have demonstrated the ability to inhibit DNA methylation in a sequence-specific fashion.

Hairpin pyrrole-imidazole (Py-Im) polyamides are a class of sequence-specific oligomers that bind in the minor groove of DNA.<sup>15-20</sup> Programmable sequence preference is accomplished by side-by-side pairings of aromatic amino acids that distinguish the edges of the four Watson-Crick base pairs.<sup>15-20</sup> Referred as the pairing rules, Im/Py codes for G•C base pairs, Hp/Py codes for T•A base pairs, and Py/Py binds both T•A/A•T in preference to G•C/C•G. Eight-ring hairpin oligomers linked by a central aliphatic  $\gamma$ -aminobutyric acid unit have affinities for match sites with  $K_a \sim 10^8$  to  $10^{10} \text{ M}^{-1}$ .<sup>16,21</sup> These binding energetics are comparable to natural transcription factors, and like natural DNA binding proteins, are sensitive to differences in the sequence-dependent microstructure of DNA. To relax the curvature of all ring hairpins,  $\beta$  alanine ( $\beta$ ) can be substituted for Py-rings in some cases such that  $\beta/\beta$  pairs replace Py/Py for T•A/A•T specificity, and Im/ $\beta$  replaces Im/Py pairs in strategic locations while retaining specificity for G•C base pair.<sup>22-</sup>

<sup>26</sup> Hairpin Py-Im polyamides usually bind with the N-to-C terminus aligned in the 5'-to-3' direction of DNA, referred to as “forward orientation”.<sup>27</sup> This modest forward binding preference can be enforced by substitution of the prochiral  $\alpha$  position in the  $\gamma$ -turn, i.e., replacement of  $\gamma$ -aminobutyric acid by (R)-2,4-diaminobutyric acid.<sup>28</sup> Hairpin architectures containing  $\beta/\beta$  pairs and  $\beta/\text{ring}$  pairs have been found in some cases to prefer the N to C terminus aligned in a 3'-to-5' direction of DNA.<sup>29</sup> While adhering to the pairing rules, this reverse hairpin orientation would bind a different DNA sequence. Recently we used massively parallel sequencing methods in conjunction with biotin-tagged hairpins, termed Bind-n-Seq, to scan genome-size DNA sequence space for



**Figure 2.1** Structure of Py-Im polyamides **S1** and **S2** previously reported to bind methylated 5'-CGCG-3' oligonucleotide duplex.<sup>32</sup> Legend for ball-and-stick notation.

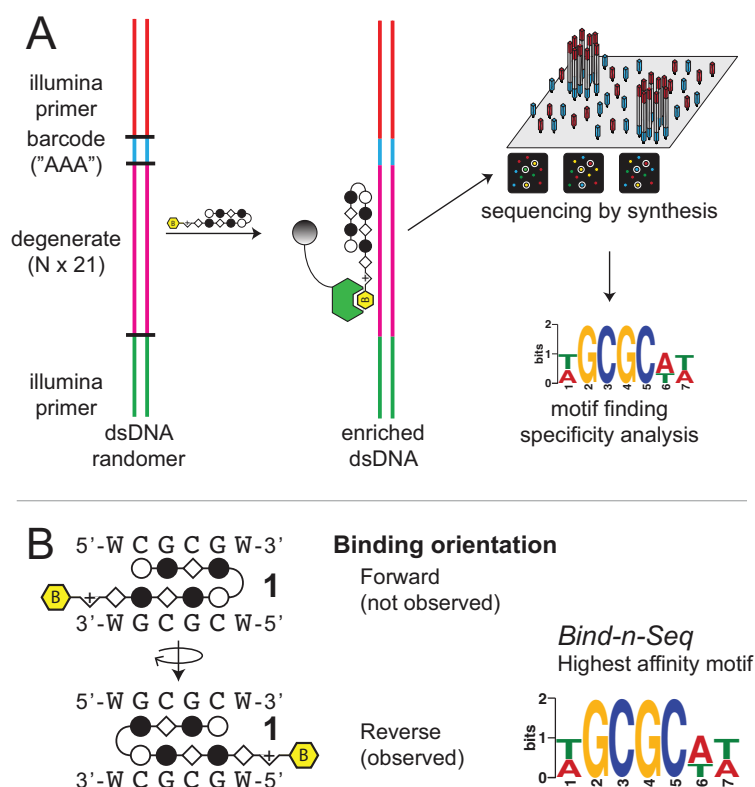
hairpin high affinity sites.<sup>30</sup> Although the canonical pairing rules are remarkably predictive of polyamide DNA binding specificity, we identified high affinity DNA binding sites in the reverse orientation for several polyamides containing β/Im pairs.<sup>30</sup>

Eight-ring hairpin Py-Im polyamides have been shown to discriminate 5'-GGGG-3', 5'-GCGC-3' and 5'-GGCC-3' with appropriate arrangement of four Im/Py pairs.<sup>31</sup> From experience, sequences with CpG steps such as 5'-CGCG-3' are not as readily accessed for reasons not well understood. In an effort to improve the affinity of an eight-ring hairpin polyamide for the sequence 5'-CGCG-3', Sugiyama and coworkers replaced two Im/Py pairs with Im/β pairs (Figure 2.1). A change from PyImPyIm-γ-PyImPyIm (**S1**) to PyImβIm-γ-PyImβIm (**S2**) afforded a 65-fold increase in affinity for 5'-CGCG-3'.<sup>32</sup> Both hairpins conform to the pairing rules and would bind 5'-CGCG-3' in the forward orientation. In this study, we employ a high-throughput sequencing assay of polyamide-DNA association to revisit targeting the 5'-CGCG-3' sequence. Our findings indicate that hairpin polyamides of sequence PyImβIm-γ-PyImβIm **S2** favor 5'-GCGC-3',

*a reverse binding mode.* The issue of designing a hairpin polyamide sequence that prefers 5'-CGCG-3' to 5'-GCGC-3' remains to be solved. Using Bind-n-Seq methods<sup>30</sup> as our screen for a library of polyamide-biotin conjugates, we find that replacement of one  $\beta$  alanine with Py to afford PyImPyIm- $\gamma$ -PyIm $\beta$ Im restores the preference for forward binding 5'-CGCG-3'. Recent structural work has shown that a cyclic Py-Im polyamide binding in the minor groove causes significant widening of the minor groove width of DNA,<sup>33,34</sup> and provides a mechanistic rationale for disruption of DNA-binding proteins in the major groove. We demonstrate the ability of our 5'-CGCG-3' specific minor groove binding hairpin polyamides to inhibit enzymatic CpG methylation in the major groove of a 5'-CGCG-3' sequence.

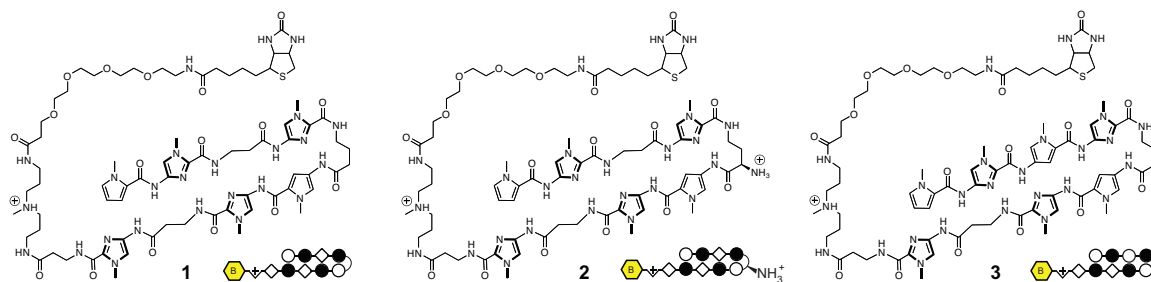
## 2.2 Results

**Sequence Based Analysis of PyIm $\beta$ Im- $\gamma$ -PyIm $\beta$ Im Specificity.** The 5'-CGCG-3' sequence is a compelling DNA target for an 8-ring hairpin Py-Im polyamide because it is one of the least represented 6-bp sequence patterns in the human genome, potentially promoting greater genomic specificity.<sup>30</sup> Minoshima and coworkers have previously targeted this sequence and shown that polyamide **S2** (Figure 2.1) can bind the fully methylated sequence.<sup>32</sup> In their study, the substitution of two  $\beta$ 's for Py moieties resulted in improved affinity for 5'-CGCG-3' over the eight-aromatic ring architecture **S1** (Figure 2.1). In light of recent Bind-n-Seq studies, however, we wondered whether these changes may have also had the unintended effect of reducing the preference of the polyamide for binding in the forward orientation.<sup>30</sup> Bind-n-Seq is a high-throughput sequencing method



**Figure 2.2** A) Scheme of Bind-n-Seq method.<sup>30</sup> Polyamide-biotin conjugate is incubated in a genome-sized library of all possible 21mers, enriched, sequenced, and the resulting dataset analyzed with motif-finding software.<sup>30</sup> B) Polyamide **1** could potentially bind in the forward orientation or the reverse orientation. The highest affinity binding sequence of **1** is the reverse orientation binding 5'-GCGC-3'.

that allows facile identification of high affinity binding sites of biotin-labeled Py-Im polyamides by affinity purification followed by sequencing (Figure 2.2A).<sup>30</sup> As a first step, we synthesized an analog of **S2** and examined polyamide-biotin conjugate **1** of sequence PyIm $\beta$ Im- $\gamma$ -PyIm $\beta$ Im (Figure 2.2B), which has a biotin affinity tag appended at the C-terminus of the heterocyclic oligomer (Figure 2.3). Polyamide-biotin conjugate **1** was incubated at 50 nM in a library of all possible 21 base pair DNA sequences,



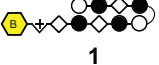

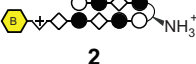

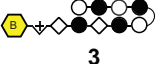

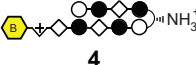

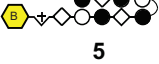

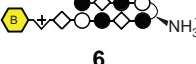

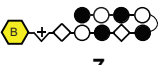

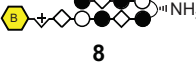
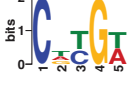
**Figure 2.3** Structures of Py-Im polyamides **1-3**.

enriched, and sequenced to identify polyamide-bound sequences. This dataset was then analyzed by the DREME algorithm to construct a motif logo summarizing the highest affinity sequences. A binding preference for 5'-GCGC-3' was revealed, suggestive of a reverse binding mode (Table 1).

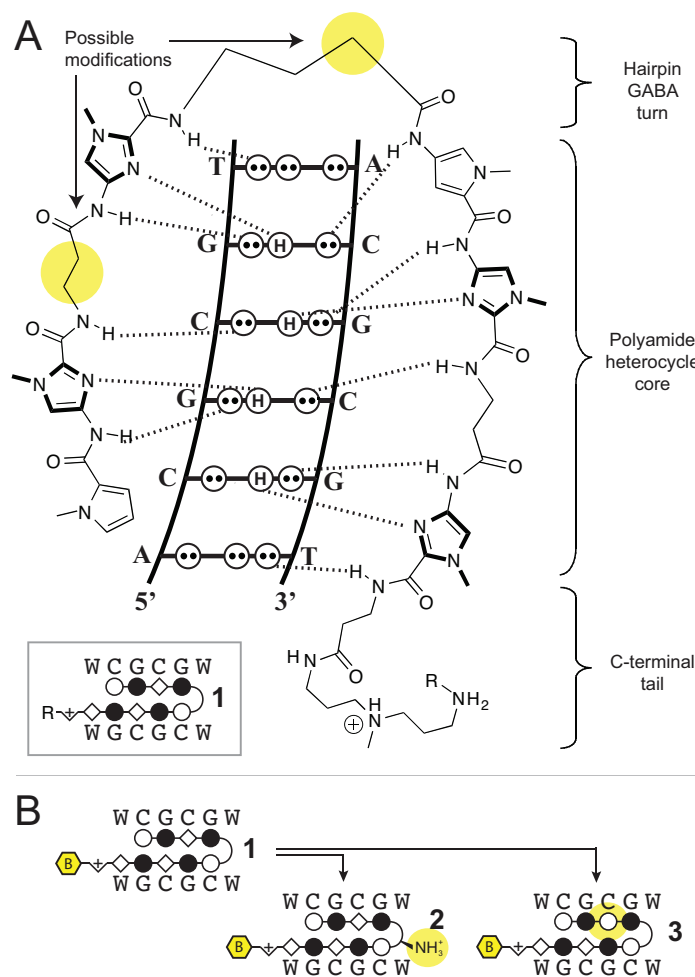
**Redesign Hairpin for CGCG versus GCGC Preference.** In order to restore the preference for binding 5'-CGCG-3' in the forward orientation, we considered two possible points of modification (Figure 2.4A). First, we made a single modification to **1** at the turn unit, replacing the GABA turn to a chiral  $\gamma$ -amino GABA, affording **2** (Figure 2.3 and 2.4B). The  $\gamma$ -amino GABA turn has previously been shown to restore forward orientation and increase affinity, including in  $\beta$ -containing polyamides.<sup>28-30</sup> This effect is thought to arise from a steric interaction with the floor of the minor groove when the chiral  $\alpha$ -amino GABA turn unit is bound in the reverse orientation.<sup>23,28</sup> Assessment of polyamide **2** by Bind-n-Seq found that this modification improved the reverse/forward ratio but was insufficient to restore a forward orientation binding preference (Table 2.1). To confirm the high-throughput sequencing findings, we performed a thermal DNA



**Table 2.1** The preferred binding orientations of polyamides **1-8** were queried with Bind-n-Seq to generate the highest affinity sequence motif. Polyamide-mediated thermal stabilization ( $\Delta T_m$ ) of 12 base pair oligonucleotides of the forward (5'-CGCG-3') and reverse 5'-GCGC-3' sequences were used to validate the revealed motifs. Melting temperatures reflect the mean and standard deviation of quadruplicate measurements.

Polyamide	Bind-n-Seq	5'-GGT <b>ACGCGT</b> ACC-3'		5'-GGT <b>AGCGCT</b> ACC-3'		Binding Orientation
		$T_m$ /°C	$\Delta T_m$ /°C	$T_m$ /°C	$\Delta T_m$ /°C	
 <b>1</b>		63.1 ( $\pm 1.0$ )	3.4	71.4 ( $\pm 0.2$ )	10.9	Reverse
 <b>2</b>		67.7 ( $\pm 0.6$ )	7.9	69.4 ( $\pm 0.3$ )	8.9	Reverse
 <b>3</b>		69.3 ( $\pm 0.4$ )	9.6	64.3 ( $\pm 0.2$ )	3.8	Forward
 <b>4</b>		67.9 ( $\pm 0.0$ )	8.1	73.2 ( $\pm 0.2$ )	12.7	Reverse
 <b>5</b>		70.3 ( $\pm 0.0$ )	9.9	67.9 ( $\pm 0.0$ )	7.7	Reverse
 <b>6</b>		68.1 ( $\pm 0.7$ )	7.7	72.6 ( $\pm 0.6$ )	12.4	Forward
 <b>7</b>		68.2 ( $\pm 0.8$ )	7.8	66.0 ( $\pm 0.2$ )	5.7	Reverse
 <b>8</b>		73.9 ( $\pm 0.7$ )	13.5	71.1 ( $\pm 0.6$ )	10.8	Reverse

denaturation study, as previous studies have shown the thermal stabilization ( $\Delta T_m$ ) of duplex DNA by Py-Im polyamides correlates well with binding affinity.<sup>35</sup> Assays were performed with DNA oligonucleotides differing only in the central binding sequence (5'-



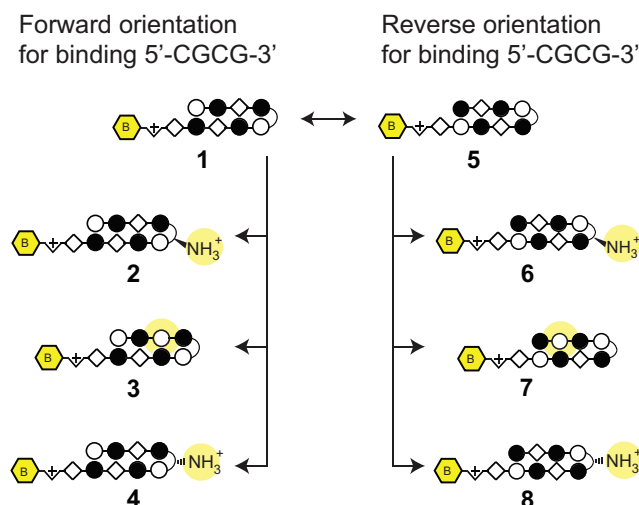
**Figure 2.4** A) Scheme of Py-Im polyamide binding in the minor groove of DNA. B) Single position changes made to hairpin polyamide **1** to afford **2** and **3**. Positions are highlighted in yellow.

CGCG-3' versus 5'-GCGC-3') to directly test the binding orientations identified by the Bind-n-Seq logos (Table 2.1). This analysis substantiated a reverse orientation binding preference for polyamide **1**, with a  $\Delta T_m$  of 10.9 °C in the reverse direction as compared to 3.4 °C in the forward direction. Modification at the turn to the  $\gamma$ -amino GABA in polyamide **2** resulted in increased stabilization of the forward 5'-CGCG-3' oligomer by 4.5 °C; stabilization by polyamide **2** in the reverse 5'-GCGC-3' orientation was diminished by 2.0 °C. This indicated an improved forward preference for 5'-CGCG-3'.

Nonetheless, the relative magnitudes of the  $\Delta T_m$  support an overall modest energetic preference for reverse orientation binding.

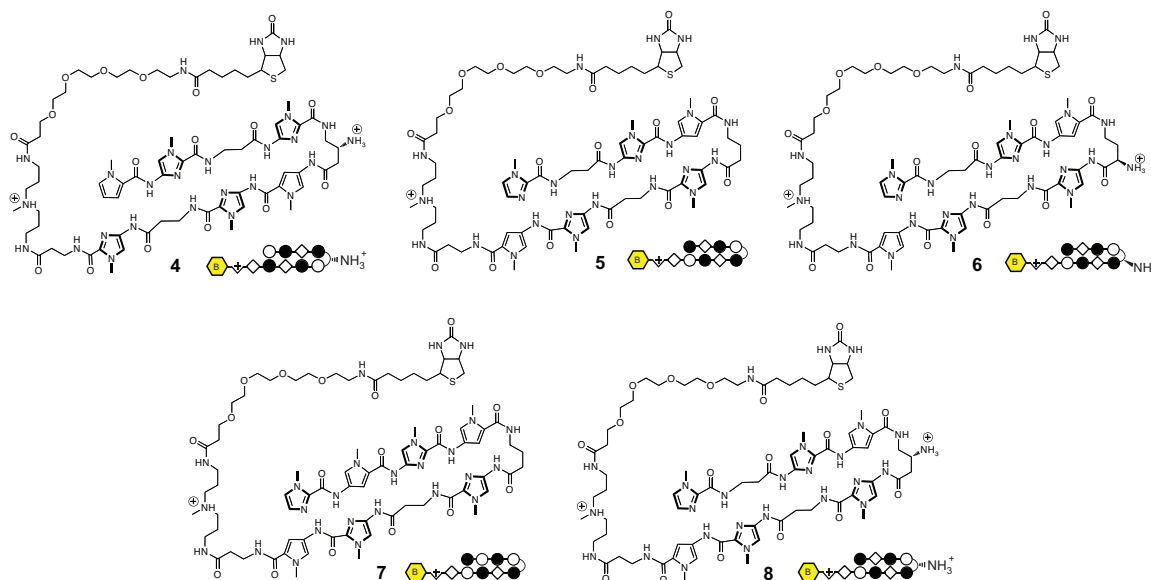
The inability of the  $\gamma$ -amino GABA turn to enforce forward orientation binding led us to investigate alternative solutions for the molecular recognition of 5'-CGCG-3'. We posited that reverse binding is abetted by the flexibility afforded by the two  $\beta$  units in the core binding region, as had been similarly noted in polyamides containing a  $\beta/\beta$  pair.<sup>29</sup> We thus considered whether removing one  $\beta$  residue might reinstitute sufficient rigidity in one of the polyamide strands to limit reverse binding while retaining the specificity and affinity provided by the other  $\beta$ . Of the two  $\beta$  moieties in the core of polyamide **1**, the C-terminal  $\beta$  in the core binding region was retained based on previous studies that have shown it is necessary for high affinity recognition of the 5' C•G base pair.<sup>24</sup> To isolate the effect of each modification, we returned to parent polyamide **1** and replaced the N-terminal  $\beta$  with a Py while retaining the achiral GABA turn, to provide polyamide **3** (Figure 2.3 and 2.4B). The assessment of **3** by Bind-n-Seq followed by DREME analysis generated a *high affinity motif consistent with forward binding 5'-CGCG-3'* (Table 2.1). This was corroborated by  $\Delta T_m$  measurements showing considerable preference for the forward 5'-CGCG-3' direction.

We further examined whether a hairpin polyamide designed to target a reverse orientation sequence may productively bind CpG's with high specificity. To test this, we



**Figure 2.5** A panel of polyamides was synthesized for assessment by Bind-n-Seq and DNA thermal stabilization for binding the 5'-CGCG-3' sequence. According to the pairing rules, polyamides **1-4** target 5'-CGCG-3' in the forward orientation and polyamides **5-8** target 5'-CGCG-3' in the reverse orientation. Structural modifications are highlighted in yellow.

expanded the library of compounds to include polyamides **4-8**, which contain single modifications targeting the 5'-GCGC/CGCG-3' core (Figure 2.5 and 2.6). In contrast to our findings with 5'-CGCG-3' targeting polyamide **2**, we confirmed that the incorporation of an  $\alpha$ -amino GABA turn in polyamide **6** restores forward orientation binding for the 5'-GCGC-3' sequence.<sup>30</sup> This difference is striking given the two polyamides are composed of nearly identical amino acid sequences. Bind-n-Seq data and  $T_m$  assays of polyamides **4**, **5**, **7**, and **8** together suggest that all other modifications preferentially bind the reverse orientation, and **5**, **7**, and **8** do so with poor specificity (Table 2.1). Indeed, amongst all variations tested of both 5'-CGCG-3' forward binding and 5'-GCGC-3' reverse binding cores, polyamide **3** displayed the highest specificity for the 5'-CGCG-3' sequence (Table 2.1).









**Figure 2.6** Structures of Py-Im polyamides 4-8.

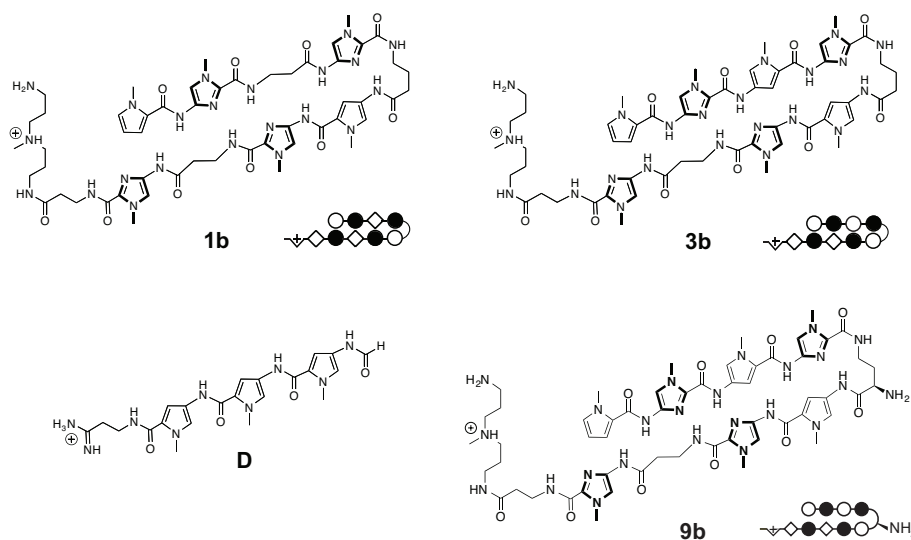
**Sequence-Specific Binding Hemi-methylated DNA.** Next, we considered the potential for minor groove binding hairpin Py-Im polyamides to prevent DNA methylation undergoing DNA replication. To do so, they must be able to bind the hemi-methylated DNA of daughter strands that have not yet undergone maintenance methylation. DNA thermal stabilization analysis was used to pursue evidence of the above trends of binding orientation with hemi-methylated DNA sequences. The sense strand of each of the 12 base pair oligomers containing 5'-CGCG-3' or 5'-GCGC-3' cores were methylated on both cytosines, whereas the antisense strand was left unmethylated. Flanking sequences were modified to lack self-complementarity and enforce hemi-methylated duplex formation. Analysis of  $\Delta T_m$  of the hemi-methylated DNA oligomers confirmed the above magnitudes of stabilization and trends of reverse and forward binding modes for **1**, **2**, and **3** (Table 2.2A).

**Inhibition of Methyltransferase.** With a specific polyamide capable of binding

**Table 2.2** A)  $T_m$  study with hemi-methylated DNA duplex. B)  $T_m$  study of three generations of 5'-CGCG-3' methylation inhibitors without biotin affinity tags.

A	Polyamide	5'-GGT <b>AC<sup>m</sup>GC<sup>m</sup>GT</b> TGG-3' 3'-CCA <b>TGC<sup>m</sup>GCA</b> ACC-5'		5'-GGT <b>AGC<sup>m</sup>GC<sup>m</sup>T</b> TGG-3' 3'-CCA <b>TCGC<sup>m</sup>GA</b> ACC-5'		Binding Orientation
		$T_m/^\circ\text{C}$	$\Delta T_m/^\circ\text{C}$	$T_m/^\circ\text{C}$	$\Delta T_m/^\circ\text{C}$	
		62.7 ( $\pm 0.5$ )	4.1	69.3 ( $\pm 1.5$ )	10.4	Reverse
		67.4 ( $\pm 0.5$ )	8.8	69.1 ( $\pm 1.2$ )	10.2	Reverse
		68.1 ( $\pm 1.0$ )	9.5	63.6 ( $\pm 1.0$ )	4.7	Forward
B	Polyamide	5'-GGT <b>ACGCGT</b> ACC-3'		5'-GGT <b>AGCGCT</b> ACC-3'		Binding Orientation
		$T_m/^\circ\text{C}$	$\Delta T_m/^\circ\text{C}$	$T_m/^\circ\text{C}$	$\Delta T_m/^\circ\text{C}$	
		67.7 ( $\pm 0.3$ )	7.1	74.1 ( $\pm 0.3$ )	13.7	Reverse
		73.6 ( $\pm 0.4$ )	13.0	68.1 ( $\pm 0.7$ )	7.7	Forward
		77.3 ( $\pm 0.6$ )	16.7	69.8 ( $\pm 0.1$ )	9.4	Forward

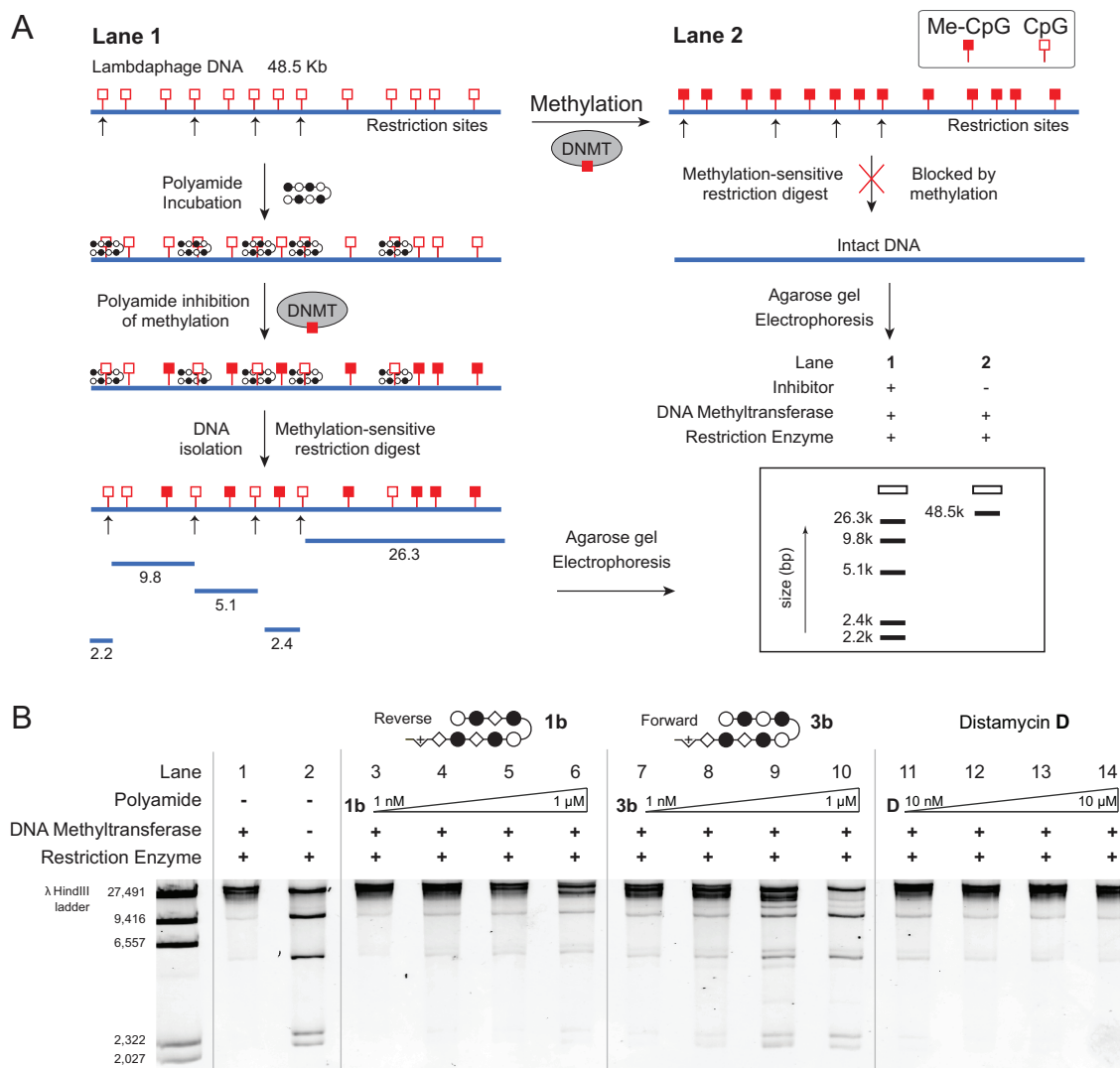
hemi-methylated DNA in hand, we evaluated its application as a sequence-specific inhibitor of DNA methyltransferases. The biotin enrichment tag was deleted from the C-terminus by re-synthesis to afford parent hairpins **1b** and **3b** (Figure 2.7). Melting temperature analyses confirmed these molecules show comparable binding preference to biotin conjugates **1** and **3**, respectively (Table 2.2B). We developed an *in vitro* assay to probe the methylation state of specific sites employing the methylation-sensitive restriction enzyme MluI to compare sequence specific effects of **1b**, **3b**, and AT-binding distamycin **D** as a control (Figure 2.8A). In this assay, we measured the ability of these



**Figure 2.7** Structures of polyamides **1b**, **3b**, **D**, and **9b** used in *in vitro* functional assays.

compounds to inhibit the methylation activity of M.SssI, a robust prokaryotic methyltransferase that operates in a processive manner like human methyltransferases and shares structural similarities with the catalytic core of human DNMT1.<sup>36</sup> We employed the methylation-sensitive enzyme MluI, which cleaves at seven 5'-ACGCGT-3' sites,<sup>37</sup> to interrogate methylation of the lambdaphage DNA (48.5 kb), of which five bands were visualized by agarose gel electrophoresis. Both **1b** and **3b** were titrated from increasing concentrations 1 nM to 1  $\mu$ M while **D** was dosed ten-fold higher from 10 nM to 10  $\mu$ M. Full digestion of the DNA by MluI indicates a lack of CpG methylation at 5'-ACGCGT-3' restriction sites, and is demonstrated by positive control lane 2 (Figure 2.8B). In contrast, full methylation would protect DNA from MluI digestion, as in lane 1, where no compound was added to DNA prior to exposure to M.SssI for methylation.

Consistent with our biophysical characterization of the compounds, polyamide **3b** showed the most robust inhibition of CpG methylation (Figure 2.8B, lanes 7-10) at



**Figure 2.8** A) Scheme of in vitro assay of DNA methyltransferase inhibition. Generic polyamide shown in ball-and-stick notation, CpG sites represented by red squares. (B) Inhibition of methyltransferase activity reflects sequence-specificity of Py-Im polyamides. Lambdaphage DNA was incubated with M.SssI and subject to methylation-sensitive restriction digest at 5'-ACGCGT-3' sites by MluI. DNA is 240 pM in match sites. Positive control lane 2 was not subject to methylation and completely digested while negative control lane 1 shows minimal digestion. Increasing concentration of 3b inhibits methylation at the restriction sites as visualized by additional, smaller restriction fragments. Polyamide 1b and 3b was titrated from 1 nM to 1 μM at ten-fold dilutions and distamycin ranged from 10 nM to 10 μM at ten-fold dilutions. Visualized on 0.7% agarose gel with SYBR gold.

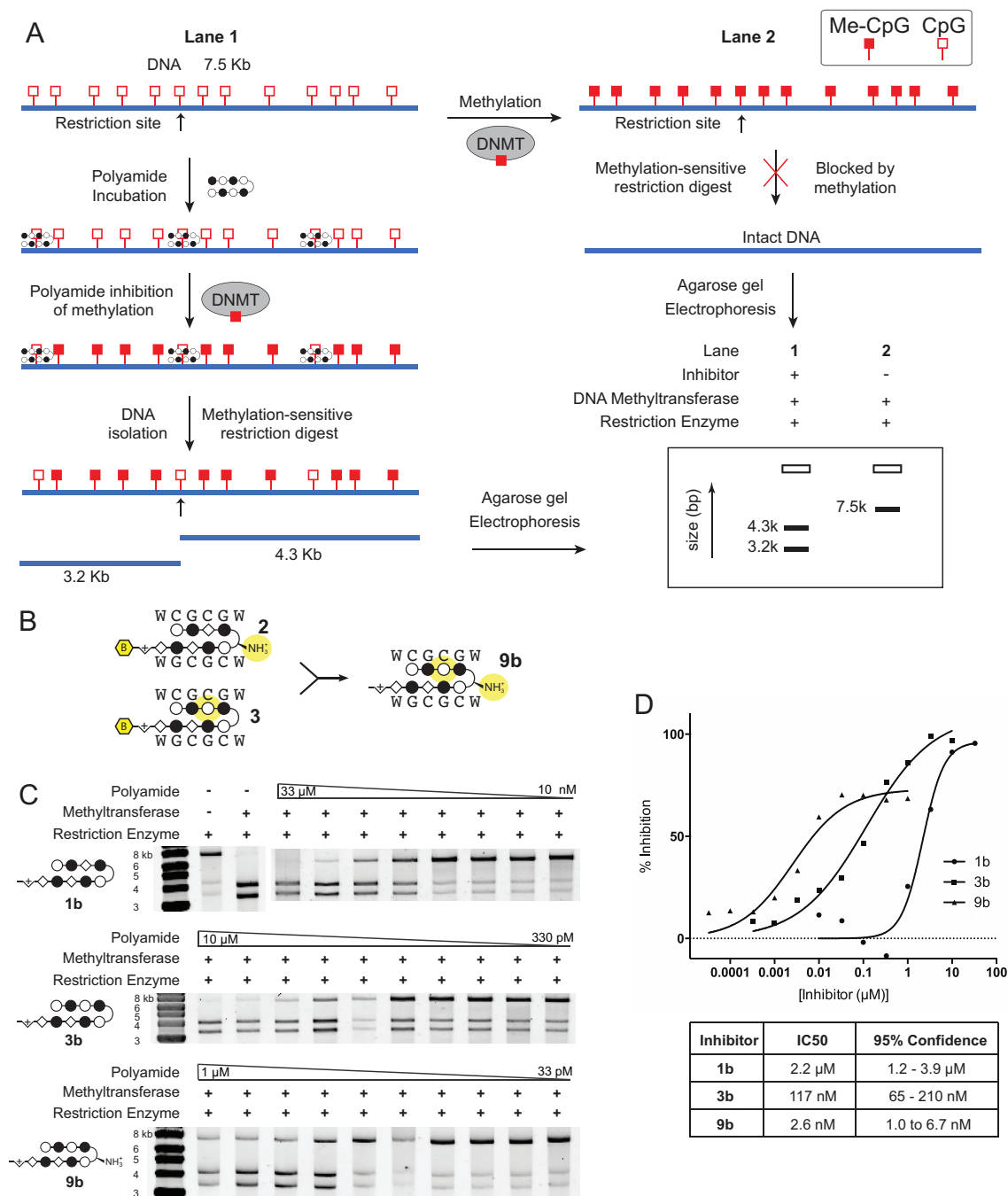
5'-ACGCGT-3' sites. In lane 10, full MluI digestion comparable to positive control lane 2 was observed at 1 μM of **3b**, indicating this concentration was sufficient to block all methylation at the cognate binding sites. Further, incomplete protection was evidenced at



100 nM of **3b** by additional, partially digested bands in lane 9. In contrast, polyamide **1b** showed weak inhibition of M.SssI and was active only at the highest concentration (Figure 2.8B, lanes 3-6). This reflects its weaker affinity for the 5'-CGCG-3' forward binding orientation, also observed by thermal duplex denaturation analysis. Inhibition by **1b** at 1  $\mu$ M, however, was reduced relative to that observed at 100 nM of **3b**, consistent with the binding preferences of the two molecules. There was no inhibition by distamycin **D** at all concentrations tested, even at the highest concentration of 10  $\mu$ M, underscoring the importance of CpG specificity of Py-Im polyamides in preventing CpG methylation. To enable quantitation of enzyme activity inhibition, the substrate DNA was changed to a 7.5 kb fragment containing a single 5'-ACGCGT-3' site (Figure 2.9A).

We were encouraged by these results to consider the design of an improved methylation antagonist at 5'-CGCG-3'. We revisited the single modifications to **1** in polyamide **2** and **3** that had promoted forward orientation binding. We combined the  $\gamma$ -amino modification at the GABA turn that had encouraged **2** to bind in the forward orientation, albeit insufficiently, with the Py substitution in the top strand, as in **3**, to afford **9b** (Figure 2.9B). Analysis by thermal denaturation assays revealed that the effects of the modifications were additive, and **9b** displayed increased affinity and preference for forward orientation binding (Table 2.2B).

We then sought to determine IC<sub>50</sub> values for the three generations of 5'-CGCG-3' methylation inhibitors: **1b**, **3b**, and **9b**. With consideration for their DNA binding



**Figure 2.9** A) Scheme of *in vitro* DNMT inhibition assay with single restriction site. Generic polyamide shown in ball-and-stick notation and CpG sites represented by red squares. DNA (7.5 kb) with a single MluI restriction site was incubated at 50 pM with inhibitor and subjected to methylation by M.SssI. DNA was isolated for restriction digest by MluI to reveal methylation at the target site. B) Single changes in polyamides **2** and **3** that promote forward orientation binding were combined in designing **9b** as a third generation candidate for improved methylation inhibition. C) Representative gel image of the polyamides **1b**, **3b**, and **9b** in the assay described in (A), suggestive of differential inhibitory activity. Dose ranges of compounds were adjusted in relation to their DNA binding affinities. D) IC<sub>50</sub> values of 5'-CGCG-3' targeting polyamides. Values are determined from band intensities in the *in vitro* assay shown in (C) and normalized

against maximal methylation with no inhibitor. IC<sub>50</sub> values were calculated from at least three replicates and fit to a four-variable, dose-response model.

affinities, compounds **1b**, **3b**, and **9b** were titrated from 10 nM to 33  $\mu$ M, 330 pM to 10  $\mu$ M, and 33 pM to 1  $\mu$ M, respectively (Figure 2.9C). It is worth noting that an additional SDS wash step was necessary in this assay to remove the higher affinity **9b** from the DNA before resolution by the MluI restriction enzyme. Prior to the addition of this SDS incubation, inhibition was maximally revealed to approximately 40%, due to polyamide inhibition of the MluI restriction enzyme. Overnight incubation of DNA in 2% SDS removed additional polyamide and improved the revealed inhibition, suggesting the compressed inhibitory range is an artifact of this method and the high affinity of **9b**. The IC<sub>50</sub> values of **1b**, **3b**, and **9b** were determined to be 2.2  $\mu$ M (95% confidence: 1.2-3.9  $\mu$ M), 117 nM (95% confidence: 65-210 nM), and 2.6 nM (95% confidence: 1.0-6.7 nM), respectively (Figure 2.9D). This is in good correlation with the iterative improvement shown in the biophysical analyses of these compounds, as well as the previous qualitative *in vitro* assay. Polyamide **9b** shows nearly 1000-fold improvement over **1b** as a 5'-CGCG-3' methylation antagonist.

## 2.3 Discussion

**Design of Antagonists of CpG Methylation.** This study provides a basis for design of sequence-specific DNA-binding molecules for targeted inhibition of CpG methylation. The disparity in methyltransferase inhibition between AT-binding distamycin **D** and hairpin polyamide **3b** suggests that the specific CpG-binding capability and widening of the minor groove by bound Py-Im polyamides are critical for disrupting DNA methylation in the major groove. At the same time, applying the pairing rules

demands caution in the design of imidazole and  $\beta$ -rich polyamides, as the inherent conformational flexibility of the  $\beta$  subunit can support unintended reverse DNA-binding modes. While previous studies have shown that an  $\beta$ -amino GABA turn unit can be used to restore the forward orientation binding preference of  $\beta$ -containing polyamides, we found 5'-CGCG-3' binding Py-Im polyamides required an alternative solution. Specifically, restoring the rigidity of the N-terminal strand via substitution of its  $\beta$ -subunit with a Py appears necessary to resolve the undesired reverse-binding of these architectures.

**Potential mechanism for inhibition of CpG methylation.** The lack of inhibition of CpG methylation by the reverse binding **1b** as compared to **3b** at the interrogated 5'-CGCG-3' sites suggests inhibition of the processive M.SssI enzyme is a sequence-specific, localized event. The M.SssI methyltransferase, like eukaryotic methyltransferases, is a “flipase” that swings the target cytosine out of the double helix and into its catalytic core.<sup>38</sup> All known CpG methyltransferases operate by this conserved mode of action. Structural studies of mouse DNMT1, the relevant mammalian methyltransferase for maintenance methylation, show that enzyme residues enter the double helix from both the major and minor grooves in an intercalative-manner around the target CpG.<sup>39</sup> These residues disrupt local base pairing and rotate the substrate cytosine around the sugar-phosphate backbone and into the catalytic core of the enzyme. A Py-Im polyamide bound to the target DNA site likely acts as a stabilizing clamp in the minor groove and prevents the intrusion of these residues. The increased DNA stability

disallows the conformational reorganization of the CpG substrate necessary for catalysis and results in the inhibition of methyltransferase activity.

## **Conclusion**

In this study, we examined programmable Py-Im polyamides targeting the 5'-CGCG-3' sequence as a model for sequence-specific inhibition of CpG methylation. The unbiased Bind-n-Seq method was critical for revealing unanticipated binding modes of the polyamides. Through deliberate, incremental synthetic modifications, we were able to discern structure activity relationships that guided improved design of CpG methylation antagonists. Further work will be necessary to understand whether this represents a more general solution for controlling Py-Im polyamide orientation or is specific to the 5'-CGCG-3' sequence. This study demonstrates that high affinity minor groove binding Py-Im polyamides can inhibit major groove CpG methylation by methyltransferase in a sequence-specific manner. It will be the focus of future research to assess these molecules as antagonists of CpG methylation in cells and its utility in the desilencing of specific genes. It will be of interest whether the intrinsic rarity of the CpG dinucleotide sequence and non-covalent binding of polyamides will reduce off-target effects.

## **2.4 Materials and methods**

**Py-Im polyamide synthesis.** Polyamides were synthesized by microwave-assisted, solid-phase synthesis on PAM resin (Peptides International) according to previously described protocols.<sup>40,41</sup> The polyamides were cleaved from resin with 3,3'-

diamino-N-methyldipropylamine and purified by reverse phase HPLC. For biotin-conjugated polyamides, the free amine at the C-terminus was allowed to react with 2

**Table 2.3** Mass Spectrometry (MALDI-TOF) for Py-Im polyamides.

Py-Im Polyamide	Formula	[Mass+H]	Found
PyImβIm-γ-PyImβImβ-(+)-PEG4-Biotin (1)	C <sub>73</sub> H <sub>108</sub> N <sub>25</sub> O <sub>17</sub> S <sup>+</sup>	1638.8	1638.0
PyImβIm-(R) <sup>α-NH<sub>2</sub></sup> γ-PyImβImβ-(+)-PEG4-Biotin (2)	C <sub>73</sub> H <sub>109</sub> N <sub>26</sub> O <sub>17</sub> S <sup>+</sup>	1653.8	1653.8
PyImPyIm-γ-PyImβImβ-(+)-PEG4-Biotin (3)	C <sub>76</sub> H <sub>109</sub> N <sub>26</sub> O <sub>17</sub> S <sup>+</sup>	1689.8	1689.2
PyImβIm-(R) <sup>β-NH<sub>2</sub></sup> γ-PyImβImβ-(+)-PEG4-Biotin (4)	C <sub>73</sub> H <sub>109</sub> N <sub>26</sub> O <sub>17</sub> S <sup>+</sup>	1653.8	1653.8
ImβImPy-γ-ImβImPyβ-(+)-PEG4-Biotin (5)	C <sub>73</sub> H <sub>108</sub> N <sub>25</sub> O <sub>17</sub> S <sup>+</sup>	1638.8	1639.0
ImβImPy-(R) <sup>α-NH<sub>2</sub></sup> γ-ImβImPyβ-(+)-PEG4-Biotin (6)	C <sub>73</sub> H <sub>109</sub> N <sub>26</sub> O <sub>17</sub> S <sup>+</sup>	1653.8	1653.9
ImPyImPy-γ-ImβImPyβ-(+)-PEG4-Biotin (7)	C <sub>76</sub> H <sub>109</sub> N <sub>26</sub> O <sub>17</sub> S <sup>+</sup>	1689.8	1690.1
ImβImPy-(R) <sup>β-NH<sub>2</sub></sup> γ-ImβImPyβ-(+)-PEG4-Biotin (8)	C <sub>73</sub> H <sub>109</sub> N <sub>26</sub> O <sub>17</sub> S <sup>+</sup>	1653.8	1654.1
PyImβIm-γ-PyImβImβ-(+)- (1b)	C <sub>52</sub> H <sub>73</sub> N <sub>22</sub> O <sub>10</sub> <sup>+</sup>	1165.6	1165.6
PyImPyIm-γ-PyImβImβ-(+)- (3b)	C <sub>55</sub> H <sub>74</sub> N <sub>23</sub> O <sub>10</sub> <sup>+</sup>	1216.6	1216.4
PyImPyIm-(R) <sup>α-NH<sub>2</sub></sup> γ-PyImβImβ-(+)- (9b)	C <sub>55</sub> H <sub>75</sub> N <sub>24</sub> O <sub>10</sub> <sup>+</sup>	1231.6	1231.7

equivalents of pre-activated PEG4-biotin NHS ester (Thermo Scientific) and 4 equivalents of DIEA for 1 hour at 55°C in DMF. The product was purified by reverse phase HPLC and lyophilized. Purity and identity of compounds were verified by analytical HPLC and matrix-assisted laser desorption/ionization time-of-flight (MALDI-TOF) mass spectrometry (Table 2.3).

**Bind-n-Seq of polyamide-biotin conjugates.** Sequence motif logos of the highest affinity DNA binding sites of polyamide-biotin conjugates **1-8** were determined

according to previously reported methods.<sup>30</sup> Each Py-Im polyamide-biotin conjugate was equilibrated at 50 nM concentration for 15 hours with a uniquely barcoded library of all possible 21mers. DNA associated with polyamide-biotin conjugates were affinity purified with streptavidin magnetic beads (M-280 Dynabeads) and eluted. Isolated DNA was amplified by touchdown PCR and sequenced at the California Institute of Technology Millard and Muriel Jacobs Genetics and Genomics Laboratory on an Illumina HiSeq 2000 Genome Analyzer. The generated dataset was then distributed by barcode using scripts in the MERMADE pipeline and a fasta file of a random 25% of sequences for each compound submitted for DREME motif analysis.<sup>30</sup>

**DNA thermal denaturation assay.** Unmethylated DNA duplexes and hairpin polyamides were mixed to a final concentration of 2 and 3  $\mu$ M, respectively, for polyamides **1-8**, **1b**, and **3b** in 1 ml total volume. For experiments with hemi-methylated oligonucleotides, DNA duplexes and hairpin polyamides were mixed to a final concentration of 1 and 1.5  $\mu$ M, respectively. An aqueous solution of 10 mM sodium cacodylate, 10 mM KCl, 10 mM MgCl<sub>2</sub>, and 5 mM CaCl<sub>2</sub> at pH 7.0 was used as analysis buffer. All oligonucleotides (100 $\mu$ M solutions dissolved in 10 mM Tris-Cl, 0.1 mM EDTA, pH 8.0) were purchased from Integrated DNA Technologies. The assay was conducted on a Varian Cary 100 spectrophotometer equipped with a thermo-controlled cell holder with a cell path length of 1 cm. Samples were heated to 90 °C and cooled to a starting temperature of 25 °C prior to heating at a rate of 0.5 °C/min to 90 °C. Denaturation profiles were recorded at  $\lambda$ = 260 nm and melting temperatures were defined as the maximum of the first derivative of the denaturation profile. Reported data represents the average of four measurements.

***In vitro* inhibition of CpG methylation assay.** In PCR tubes, serially diluted concentrations of polyamides **1b**, **3b**, and distamycin **D** control were incubated in 96  $\mu$ l of 10 pM unmethylated lambdaphage DNA (Promega) and 1X NEB2 buffer (New England Biolabs) in DEPC-treated water (USB) for 12 hours at 25 °C. Two additional samples of DNA in buffer without compound were kept for controls. After incubation, S-adenosyl methionine (New England Biolabs) and M.SssI (New England Biolabs) or water was added to all samples to a final concentration of 320  $\mu$ M and 0.25 Units, respectively, to afford 100  $\mu$ l of total solution. Samples were then incubated for 3 hours at 37 °C on a Biorad MyCycler thermal cycler and heat inactivated for 15 minutes at 65 °C. DNA was ethanol precipitated in a centrifuge at 4 °C for 15 minutes with the addition of 10  $\mu$ l of 3M NaOAc, 1  $\mu$ l of glycogen, and 2.5 volumes of ethanol at -20 °C. DNA was washed once with 75% aqueous ethanol at -20 °C and allowed to air dry for 30 minutes. Samples were dissolved in 35  $\mu$ l of water and 15  $\mu$ l taken for MluI restriction enzyme digestion. Samples were prepared in PCR tubes per manufacturer's protocol with 1 Unit of MluI per sample and incubated at 37 °C for 1 hour. Blue loading buffer 6x (New England Biolabs) was added to samples and 20  $\mu$ l added to a 0.7% agarose gel in 0.5x TBE buffer. DNA was visualized with SYBR gold (Invitrogen) and a Typhoon FLA9000 Scanner (GE Healthcare).

**Determination of IC<sub>50</sub>.** The *in vitro* assay was run as described above with **1b**, **3b**, and **9b** at concentrations titrated at 10-fold and 3-fold intervals ranging from 10 nM to 33  $\mu$ M, 330 pM to 10  $\mu$ M, and 33 pM to 1  $\mu$ M, respectively, and DNA at 50 pM. The substrate DNA fragment (7.5 kb) was PCR amplified from PTYB21 (New England Biolabs) after linearization with BamHI (New England Biolabs). Primers 5'-



ACTTTTCGGGGAAATGTGCG-3' and 5'-TTAGAGGCCCCAAGGGGTTA-3' (IDT DNA) were used for amplification with the Expand Long Template PCR System (Roche). The amplicon was isolated with QIAquick PCR Purification Kit (Qiagen), and the amplicon size was verified by agarose gel electrophoresis. After the ethanol precipitation step, which follows methylation, the DNA pellet was dissolved in 100 µl of 2% SDS and incubated overnight at 55 °C to wash off residual polyamide. The high affinity of **9b** made this additional wash step necessary prior to MluI digestion. To the solution, 10 µl of 2M NaCl followed by 2.5 volumes of ethanol were added to re-precipitate the DNA. The pellet was washed twice with cold 75% ethanol before submission to MluI digest, as described above. Digested samples were run on 1% agarose gels and visualized with SYBR Gold. Gels were scanned on a Typhoon FLA Scanner (GE Healthcare) and the bands quantitated using ImageQuant Software (GE Healthcare). Percentage inhibition was normalized against maximal methylation in the presence of no inhibitor.

$$\% \text{ Inhibition} = 100\% \times \left(1 - \frac{\% \text{ uncut DNA}}{\% \text{ Maximal uncut DNA}}\right)$$

IC50 curves and 95% confidence intervals were determined using GraphPad Prism by variable-slope, nonlinear regression fit to a dose response model with a bottom constraint of 0. At least three replicates of each concentration were used.

## 2.5 Acknowledgment

Sequencing was conducted at the Millard and Muriel Jacobs Genetics and Genomics Laboratory at the California Institute of Technology. Mass spectrometry analyses were performed in the Mass Spectrometry Laboratory of the Division of

Chemistry and Chemical Engineering at the California Institute of Technology. Gels were scanned in the Center for the Chemistry of Cellular Signaling at the California Institute of Technology. Studies were funded in part by the National Institutes of Health (grant numbers GM51747 and GM27681); Tobacco-Related Disease Research Program (award number 20DT-0037 to J.S.K., dissertation research award); and American Cancer Society (grant number PF-10-015-01-CDD to J.L.M., postdoctoral fellowship).

## 2.6 References

- (1) Jones, P. A.; Baylin, S. B. *Nat. Rev. Genetics* **2002**, *3*, 415-428.
- (2) Rountree, M. R.; Bachman, K. E.; Herman, J. G.; Baylin, S. B. *Oncogene* **2001**, *20*, 3156-3165.
- (3) Bird, A. P. *Nature* **1986**, *321*, 209-213.
- (4) Ballestar, E.; Wolffe, A. P. *Eur. J. Biochem.* **2001**, *268*, 1-6.
- (5) Merlo, A.; Herman, J. G.; Mao, L.; Lee, D. J.; Gabrielson, E.; Burger, P. C.; Baylin, S. B.; Sidransky, D. *Nat. Med.* **1995**, *1*, 686-692.
- (6) Katzenellenbogen, R. A.; Baylin, S. B.; Herman, J. G. *Blood* **1999**, *93*, 4347-4353.
- (7) Plumb, J. A.; Strathdee, G.; Sludden, J.; Kaye, S. B.; Brown, R. *Cancer Res.* **2000**, *60*, 6039-6044.
- (8) Dammann, R.; Li, C.; Yoon, J. H.; Chin, P. L.; Bates, S.; Pfeifer, G. P. *Nat. Genet.* **2000**, *25*, 315-319.
- (9) Christman, J. K. *Oncogene* **2002**, *21*, 5483-5495.
- (10) Waring, M. J.; Wakelin, L. P. G. *Nature* **1974**, *252*, 653-657.
- (11) Adams, R. L.; Rinaldi, A. *FEBS Lett.* **1987**, *215*, 266-268.
- (12) Stresemann, C.; Brueckner, B.; Musch, T.; Stopper, H.; Lyko, F. *Cancer Res.* **2006**, *66*, 2794-2800.
- (13) Fagan, R. L.; Cryderman, D. E.; Kopelovich, L.; Wallrath, L. L.; Brenner, C. *J Biol. Chem.* **2013**, *288*, 23858-23867.
- (14) Ceccaldi, A.; Rajavelu, A.; Ragozin, S.; Sénamaud-Beaufort, C.; Bashtrykov, P.; Testa, N.; Dali-Ali, H.; Maulay-Bailly, C.; Amand, S.; Guianvarch, D. *ACS Chem. Biol.* **2013**, *8*, 543-548.
- (15) Wade, W. S.; Mrksich, M.; Dervan, P. B. *J. Am. Chem. Soc.* **1992**, *114*, 8783-8794.
- (16) Trauger, J. W.; Baird, E. E.; Dervan, P. B. *Nature* **1996**, *382*, 559-561.
- (17) White, S.; Baird, E. E.; Dervan, P. B. *Chem. Biol.* **1997**, *4*, 569-578.

- (18) White, S.; Szewczyk, J. W.; Turner, J. M.; Baird, E. E.; Dervan, P. B. *Nature* **1998**, *391*, 468-471.
- (19) Kielkopf, C. L.; Baird, E. E.; Dervan, P. B.; Rees, D. C. *Nat. Struct. Biol.* **1998**, *5*, 104-109.
- (20) Kielkopf, C. L.; White, S.; Szewczyk, J. W.; Turner, J. M.; Baird, E. E.; Dervan, P. B.; Rees, D. C. *Science* **1998**, *282*, 111-115.
- (21) Mrksich, M.; Parks, M. E.; Dervan, P. B. *J. Am. Chem. Soc.* **1994**, *116*, 7983-7988.
- (22) Trauger, J. W.; Baird, E. E.; Mrksich, M.; Dervan, P. B. *J. Am. Chem. Soc.* **1996**, *118*, 6160-6166.
- (23) Swalley, S. E.; Baird, E. E.; Dervan, P. B. *Chem. Eur. J.* **1997**, *3*, 1600-1607.
- (24) Trauger, J. W.; Baird, E. E.; Dervan, P. B. *J. Am. Chem. Soc.* **1998**, *120*, 3534-3535.
- (25) Turner, J. M.; Swalley, S. E.; Baird, E. E.; Dervan, P. B. *J. Am. Chem. Soc.* **1998**, *120*, 6219-6226.
- (26) Wang, C. C.; Ellervik, U.; Dervan, P. B. *Bioorg. Med. Chem.* **2001**, *9*, 653-657.
- (27) White, S.; Baird, E. E.; Dervan, P. B. *J. Am. Chem. Soc.* **1997**, *119*, 8756-8765.
- (28) Herman, D.; Baird, E.; Dervan, P. B. *J. Am. Chem. Soc.* **1998**, *120*, 1382-1391.
- (29) Rucker, V.; Melander, C.; Dervan, P. *Helv. Chim. Acta* **2003**, *86*, 1839-1851.
- (30) Meier, J. L.; Yu, A. S.; Korf, I.; Segal, D. J.; Dervan, P. B. *J. Am. Chem. Soc.* **2012**, *134*, 17814-17822.
- (31) Swalley, S. E.; Baird, E. E.; Dervan, P. B. *J. Am. Chem. Soc.* **1997**, *119*, 6953-6961.
- (32) Minoshima, M.; Bando, T.; Sasaki, S.; Fujimoto, J.; Sugiyama, H. *Nucleic Acids Res.* **2008**, *36*, 2889-2894.
- (33) Chenoweth, D. M.; Dervan, P. B. *Proc. Natl. Acad. Sci. U.S.A* **2009**, *106*, 13175-13179.
- (34) Chenoweth, D. M.; Dervan, P. B. *J. Am. Chem. Soc.* **2010**, *132*, 14521-14529.
- (35) Pilch, D. S.; Poklar, N.; Gelfand, C. A.; Law, S. M.; Breslauer, K. J.; Baird, E. E.; Dervan, P. B. *Proc. Natl. Acad. Sci. U.S.A* **1996**, *93*, 8306-8311.

- (36) Brueckner, B.; Garcia Boy, R.; Siedlecki, P.; Musch, T.; Kliem, H. C.; Zielenkiewicz, P.; Suhai, S.; Wiessler, M.; Lyko, F. *Cancer Res* **2005**, *65*, 6305-6311.
- (37) McClelland, M.; Nelson, M. *Nucleic Acids Res.* **1992**, *20 Suppl*, 2145-2157.
- (38) Darii, M. V.; Cherepanova, N. A.; Subach, O. M.; Kirsanova, O. V.; Raskó, T.; Slaska-Kiss, K.; Kiss, A.; Deville-Bonne, D.; Reboud-Ravaux, M.; Gromova, E. S. *Biochim Biophys Acta* **2009**, *1794*, 1654-1662.
- (39) Song, J.; Teplova, M.; Ishibe-Murakami, S.; Patel, D. J. *Science* **2012**, *335*, 709-712.
- (40) Baird, E. E.; Dervan, P. B. *J. Am. Chem. Soc.* **1996**, *118*, 6141-6146.
- (41) Puckett, J. W.; Green, J. T.; Dervan, P. B. *Org. Lett.* **2012**, *14*, 2774-2777.